Critical Review

Structure and Function of Yeast and Fungal Na^+/H^+ Antiporters

Debajyoti Dutta
Larry Fliegel*

Department of Biochemistry, University of Alberta, Edmonton, AB, Canada

Abstract

Sodium proton antiporters (or sodium proton exchangers [NHEs]) are a critical family of membrane proteins that exchange sodium for protons across cell membranes. In yeast and plants, their primary function is to keep the sodium concentration low inside the cytoplasm. One class of NHE constitutively expressed in yeast is the plasma membrane Na^+/H^+ antiporter, and another class is expressed on the endosomal/vacuolar membrane. At present, four bacterial plasma membrane antiporter structures are known and nuclear magnetic resonance structures are available for the membrane spanning transmembrane helices of mammalian and yeast NHEs. Additionally, a vast amount of mutational data are available on the role of individual amino acids and critical motifs involved in transport. We combine this information to obtain a more detailed picture of the yeast NHE plasma membrane protein and review mechanisms of transport, conserved motifs, unique residues important in function, and regulation of these proteins. The Na^+/H^+ antiporter of *Schizosaccharomyces pombe*, *Sp*NHE1, is an interesting model protein in an easy to study system and is representative of fungal Na^+/H^+ antiporters. © 2017 IUBMB Life, 70(1):23–31, 2018

Keywords: *cation coordination; Na^+/H^+ antiporter; Na^+/H^+ exchanger; salt tolerance; yeast*

INTRODUCTION

In yeast, alkali metal homeostasis is critical to cell growth and survival. A high level of intracellular potassium and a relatively low level of intracellular sodium are important to maintain normal metabolic activity. Potassium channels, H^+-ATPase, Na^+-K^+-ATPase, and sodium (or potassium) proton exchangers (antiporters) (or sodium proton exchangers [NHEs]) are the major membrane transport proteins that maintain yeast cytosol ion homeostasis. Most plasma membrane antiporters use the energy of the proton gradient generated by the activity of the H^+-ATPase to remove Na^+ from cytoplasm. Excessive intracellular sodium is toxic to yeast and NHEs are constitutively expressed proteins that provide alkali metal tolerance (1).

Yeast that possess well-characterized NHE proteins are *Saccharomyces cerevisiae* and *Schizosaccharomyces pombe*. *S. cerevisiae* grow in up to molar concentrations of sodium and have several proteins contributing to sodium tolerance. This includes the plasma membrane efflux proteins: Na^+-ATPases, Pi-Na^+ symporter Pho89, and Nha1p, a Na^+/H^+ antiporter (1). Intracellular transporters also contribute to salt tolerance and are comprised of vacuolar cation/proton antiporters, and transporters of the endosomes and Golgi apparatus (here only dealt with briefly). *Zygosaccharomyces rouxii* is another related species of yeast which has been well studied and whose proteins involved in salt tolerance has been characterized (and is reviewed here where appropriate).

From a scientific point of view, *S. pombe* is an ideal system to study the structure and function of plasma membrane salt tolerance proteins. *S. pombe* has only one major NHE in its plasma membrane and does not have a Na^+-ATPase in its genome that expels Na^+ (2). Early work (2) demonstrated that the knockout of *S. pombe* NHE1 (*Sp*NHE1, originally referred

Additional Supporting Information may be found in the online version of this article.

Abbreviations: *NhaA, Na^+/H^+ antiporter type A; NHE, Na^+/H^+ exchanger; NHX, vacuolar Na^+/H^+ exchanger; NMR, nuclear magnetic resonance; TM, transmembrane*

Volume 70, Number 1, January 2018, Pages 23–31

**Address correspondence to: Larry Fliegel, Department of Biochemistry, 347 Medical Science Building, University of Alberta, Edmonton, Alberta, Canada T6G 2H7. Tel: 780-492-1848. Fax: 780-492-0886. E-mail: lfliegel@ualberta.ca*

Received 26 October 2017; Accepted 21 November 2017

DOI 10.1002/iub.1701

Published online 8 December 2017 in Wiley Online Library (wileyonlinelibrary.com)

to as sod2) results in a salt sensitive phenotype. Return of this gene restores salt tolerance. This allows the indirect assay of *Sp*NHE1 by assay of *S. pombe* growth in salt containing media (3–5). Other plasma membrane NHEs such as *S. cerevisiae* Nha1p (*Sc*Nha1p) and *Z. rouxii* Sod2 (*Zr*Sod2p) have also been characterized to varying degrees (6–8). *Sp*NHE1 shares 42% and 43% identity with *Sc*Nha1p and *Zr*Sod2p and 66% and 54% similarity, respectively (9).

While the entire structure of any yeast plasma membrane Na^+/H^+ antiporter is not known, in some bacteria, the crystal structures of plasma membrane Na^+/H^+ antiporters have been deduced, that of *Escherichia coli*, NhaA (10), NapA of *Thermus thermophilus* (11), *Mj*NhaP1 of *Methanocaldoccocus jannaschii* (12), and PaNhaP of *Pyrococcus abyssi* (13) (summarized in Supporting Information Table S1). This has led to the development of the idea that Na^+/H^+ antiporters have a novel fold (NhaA fold) or assembly, consisting of two pairs of short helices that are connected by crossed, extended non-helical chains. The structure of mammalian Na^+/H^+ exchangers has not been deduced, although nuclear magnetic resonance (NMR) structures of isolated transmembrane (TM) segments of human Na^+/H^+ exchanger isoform 1 (*h*NHE1) have been reported (14–19). Structural information of two critical TM segments of *Sp*NHE1 has also been reported (5). However, despite the presence of this structural data, few correlations have been made between this data and mutational effects in Na^+/H^+ antiporters of yeast species.

Soil salinity is a major factor in reducing plant growth and productivity (20). The degree of salt tolerance of some plant species varies greatly (21) and expression of *Sp*NHE1 has been shown to increase the salt tolerance of *Arabidopsis thaliana* (22). SOS1 is the plasma membrane Na^+/H^+ antiporter of *Arabidopsis* and in the membrane domain it has 24% identity and 38% similarity to *Sp*NHE1 (unpublished observation).

In this article, we review and identify present knowledge of critical residues in the TM domains of yeast plasma membrane Na^+/H^+ antiporters, with emphasis on *Sp*NHE1. Comparisons are made, where appropriate, to Na^+/H^+ antiporters whose 3D structure is known and to SOS1, *h*NHE1, and other yeast Na^+/H^+ antiporters (Supporting Information Table S1). Additionally, we present a revised predicted model of the structure of yeast plasma membrane *Sp*NHE1. We also discuss the possible role of conserved residues and motifs in the light of present structural and functional data. The accumulated knowledge may be extended to help understand the mechanism of Na^+/H^+ antiport across plasma membranes, and to help develop salt tolerant versions of yeast plasma membrane Na^+/H^+ antiporters for commercial development.

DIVERSITY AND FUNCTION

There are different types of cation proton antiporters in the yeast genome. Based on localization, they can be grouped into two categories: plasma membrane antiporters and intracellular antiporters. Intracellular cation proton antiporters (reviewed below) include the vacuolar Na^+/H^+ antiporters (Nhx) and are usually broad-spectrum antiporters sharing high sequence identity (23). Classification of yeast cation proton antiporters can also be based on substrate specificity. Two groups can be distinguished, one with narrow substrate specificity (like *Sp*NHE1 for Na^+ and Li^+), and a second broad substrate specificity group which may transport as least four alkali metal cations, Na^+, Li^+, K^+, and Rb^+ (24).

The number of cation proton antiporters encoded by yeast genomes varies from one species to another (9). The *S. cerevisiae* genome contains three genes Nha1, Nhx1, and Kha1. Nhx1p is a Na^+/H^+ antiporter that enhances salt tolerance by moving cations to intracellular compartments (Supporting Information Table S1). *Sc*Nhx1p is distributed in multiple organelles including trans-Golgi network compartments, late and recycling endosomes (25). The protein is more characterized than some other family members. It regulates luminal and cytoplasmic pH, which controls vesicle trafficking out of endosomes and fusion. It transports both K and Na (26,27). *Sc*Nhx1p (28) possesses N-linked glycosylation that, unusually, map to the C-terminal tail domain. The membrane domain of the protein is proposed to contain 12 TM segments with TM 1 serving as a putative signal sequence (28). Among other cation proton antiporters, *Sc*Kha1p is localized in the Golgi where it may play a role in cell growth at alkaline pH levels. *Sc*Nha1p is at the plasma membrane and has broad substrate specificity, possibly regulating intracellular pH (9). In the *Z. rouxii* genome, there is diversity in copy numbers depending on the strain. One *Z. rouxii* strain contains Nha1-like antiporters *Zr*Nha1 and *Zr*Sod22, whereas only one copy is present in another strain (9,29) (Supporting Information Table S1). *S. pombe* also contains two plasma membrane Na^+/H^+ antiporters, *Sp*NHE1 and *Sp*Sod22. *Sp*NHE1 is specific for both Li^+ and Na^+ and its deletion results in a sodium and lithium sensitive phenotype (2). *Sp*Sod22 is a broad-spectrum antiporter with both Na^+ and K^+ specificities but it works less efficiently for Na^+ and may be involved in tolerance to K^+, especially at lower external pH (30).

Pribylova et al. (9) reported the presence of another member of the Nhx1 cation/proton antiporter family present in *S. pombe* (Supporting Information Table S1). It had high levels of identity to other members of the Nhx family. This Nhx1 protein is thought to be prevacuolar/endosomal and is related to human intracellular and vacuolar plant antiporters (9,23).

PROTEIN STRUCTURE

Structure of the Membrane Domain

The structure of the membrane domains of the plasma membrane Na^+/H^+ antiporters was revealed in crystallized proteins and has significant diversity. *Ec*NhaA contains 12 TM helices per protomer with both N- and C-terminal cytoplasmic tails. It has two distinct subdomains: a dimerization or scaffolding subdomain and a cylindrical or six-helix bundle transport subdomain (10,31). The structures of three other plasma membrane Na^+/H^+

antiporters *Pa*NhaP, *Tth*NapA, and *Mj*NhaP1 (11,13,32), show diversity from *Ec*NhaA. These structures contain 13 TM helices with the extra TM helix at the N-terminal believed to act as an uncleaved signal sequence that also affects allosteric regulation of antiporter activity (32). For *Tth*NapA, it was shown that the topology is N-terminal out and C-terminal in (11).

The *h*NHE1 topology has been debated. An early study (33) used cysteine scanning accessibility and suggested a 12-TM segment model. Later, an alternative 3D model was proposed based on the structure of *Ec*NhaA (34). This model also had 12 TM helices although with several notable differences in assignment of the first TM segment and amino acids 315–411. A subsequent article (35) supported the original report (33); however, a definitive 3D structure for this protein is lacking.

The topology of *At*SOS1 has not been elucidated experimentally. A recent (36) prediction was that SOS1 has 13 TM segments, similar to the topologies of *Pa*NhaP, *Tth*NapA, and *Mj*NhaP1 and divergent from *Ec*NhaA.

The membrane domains of the plasma membrane Na^+/H^+ antiporters have a domain-like structure (37). *Ec*NhaA has two distinct subdomains called the interfacial or scaffolding domain and the ion translocation domain, each of which is a six alpha helix bundle, made up of two or three TM bundles. The overall structure of *Tth*NapA (11) is quite similar to that of *Ec*NhaA differing in an extra helix (termed −1) and the position of the core relative to the dimerization domain (31). *Mj*NhaP1 (32) was modeled and fit as conserved six helix bundles based on NhaA and *Pa*NhaP (13) and was also an inverted six helix repeat.

NHE Oligomerization

Na^+/H^+ antiporters are dimers. The dimerization axis is perpendicular to the plane of the membrane bilayer. The best characterized dimerization is that of *E. coli* NhaA. The *Ec*NhaA structure has dimer contacts where extracellular beta strands and TM 1, TM 9, TM 6, and TM 7 are involved. Helices 6 and 7 form an alpha hairpin at the dimer interface. Deletion of these TM segments causes defective dimerization, assembly, and stability, although the protein still retains significant transport activity (38). In *Ec*NhaA, a beta sheet on the periplasmic side of the membrane is also important in dimerization. Its deletion leaves a functional protein that can confer salt tolerance, although with reduced efficiency (39).

*Mj*NhaP1 is also a dimer but the dimer contacts are quite different from *Ec*NhaA. The protomers are held together by tight helix–helix interactions across an extensive, probably hydrophobic, contact surface at the dimer interface. There is no evidence of a periplasmic beta sheet. When TM 1 of *Mj*NhaP1 is deleted, the protein can still make a stable dimer but is devoid of transport activity (32).

Eukaryotic NHEs are also homodimers, which was shown both chemically (40) and by examining the assembly of human NHE1 using cryoelectron microscopy (41). The electron micrograph was indicative of a dimer where the dimerization of the membrane domains is also assisted by the long C-terminal cytoplasmic domain (41). A similar homodimer assembly was found in the plant plasma membrane Na^+/H^+ antiporter *A. thaliana* SOS1 (42), where it was suggested that the dimerization was stabilized by both the membrane domain and the large cytosolic domain. Supporting this suggestion was the observation that expressed and purified C-terminal of SOS1 can make an intermolecular disulphide bond (36). There has been little work in this area on *Sp*NHE1, however earlier, we expressed *Sp*NHE1 and demonstrated that it is a dimer by crosslinking experiments (43).

Extramembrane Domains

Yeast and fungal plasma membrane cation proton antiporters vary in terms of total amino acid length but the number of amino acids in the membrane domain is fairly consistent, often 397 to 426 amino acids (9). Earlier studies (9) suggested that most yeast transporters have a prediction of an even number of TM segments, 10 to 12, although there was little experimental support for these computer predictions. The antiporter families of yeast Nhx1p, Kha1p, and Nha1p were thought to have short hydrophilic N-termini ranging generally from 13 to 61 residues. In contrast, the length of C-terminal cytoplasmic domains varies greatly. For *Sc*Nha1p, it consists of amino acids 438–985 and plays a role in regulation of activity (44,45). The protein can target to the plasma membrane with only 438 amino acids (46). Some regions of the tail are activating and aid in responses to changes in osmolarity (44,45). Hog1 MAP kinase phosphorylates *Sc*Nha1p and stimulates activity (47). A yeast homolog of 14-3-3, bmh1, binds to *Sc*Nha1p and enhances resistance to salt stress (47). The 14-3-3 proteins are known to bind to phosphoproteins. Although, in this case, the binding of 14-3-3 to *Sc*Nha1p was not dependent on Hog1 MAP kinase. Other kinases could be responsible for phosphorylation that promotes 14-3-3 binding (48). Another membrane protein, COS3, also interacts with the proximal region of the *Sc*Nha1p tail enhancing salinity-resistant cell growth (49). Interestingly, the extreme C-terminal region of the tail (amino acids 945–985) has an autoinhibitory effect and its deletion is stimulatory.

Other plasma membrane antiporters also have large C-terminal regions. In Sod2–22p of *Z. rouxii* the C-terminus is over 350 amino acids in length (9). In *At*SOS1, the membrane domain ends at amino acid 440, while the balance of the 1,146 amino acids is a regulatory domain that includes an autoinhibitory domain and sites for regulation by phosphorylation (50). Mammalian *h*NHE1 has a 315 amino acid C-terminal regulator tail that is subject to regulation by phosphorylation and protein binding (51). It is known to be partially disordered and phosphorylation and protein binding alters its conformation and regulatory properties (37,52). *Sp*NHE1 only has 30–40 C-terminal tail amino acids (2,53).

NhaA Fold

As noted above, the first Na^+/H^+ antiporter crystal structure contained what has been called the "*Ec*NhaA fold" (31). This is a catalytic region at the middle of membrane, which consists of antiparallel unfolded regions that cross each other forming a delicate electrostatic balance mid membrane. Charged and polar residues

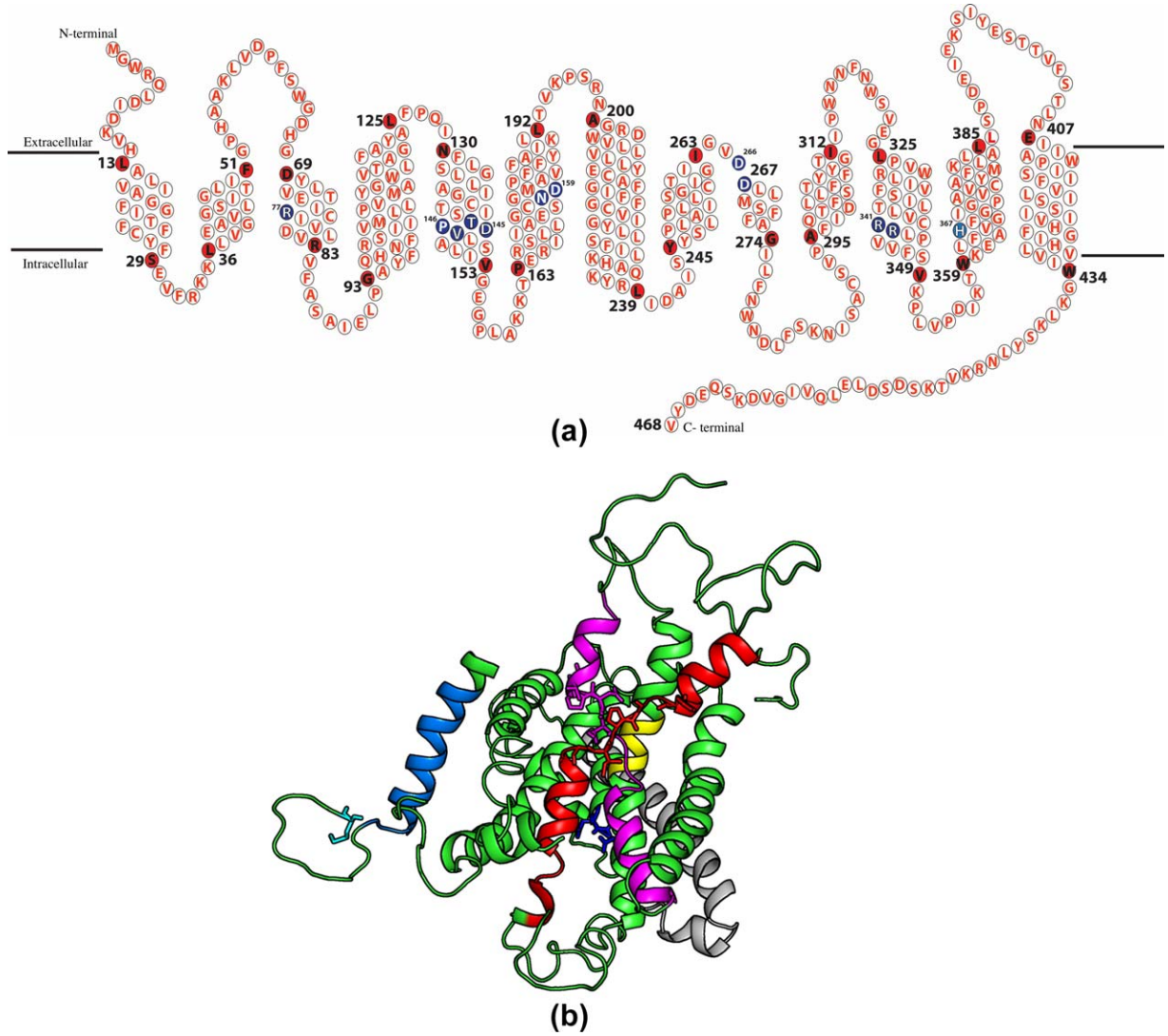

FIG 1

Structural models of Sp*NHE1. (A) Predicted topology of* Sp*NHE1 derived from molecular model predictions. Residues highlighted in red indicated putative boundaries of the membrane domain. Other residues forming conserved amino acids or important motifs, discussed in the text, are highlighted in blue, Arg77, ^{144}TDPV^{147}, ^{158}ND^{159}, ^{266}DD^{267}, ^{341}RR^{342}, and His367. (B) Three-dimensional topology of* Sp*NHE1 based on homology model of* Sp*NHE1 with* Pa*NhaP structure as described in the text. TM 5, magenta with amino acid side chains ^{144}TDPV^{147} shown; TM 12, red, with amino acid side chains of ^{369}GPIG^{372} and His367 shown; TM 11 (325–349), TM 2 (34–49), and TM 13 (409–437) were removed for clarity, ^{1}Met, blue; ^{173}EXXXND^{178} shown in yellow; TM 1, blue; TM 8, grey.*

may play a role in neutralizing the helix dipoles. Interestingly, the unwound portion of TM 4 undergoes a conformational change with varying physiological pH and lines the cation passage (54). This structure contributes to the cation binding site and allows for rapid conformational changes that occur in transport. This fold is shared by *Tth*NapA (11), *Mj*NhaP1 (32), and *Pa*NhaP, which also have discontinuous helices 5 and 12, which correspond to 4 and 11 of *Ec*NhaA (13).

The crystal or cryoelectron microscopic structure of full-length *h*NHE1 has not been deduced. However, several studies have examined the structure of TM segments of *h*NHE1 by NMR, and these structures have a good agreement with crystal structures of proteins (55). TM 4 (17) contained an extended region in the mid membrane region and had a rough similarity in structure to TM 4 of *Ec*NhaA, although amino acid identity was low between the two proteins. Similarly, TM 11 of *h*NHE1 has a helix-extended region-helix structure that is similar to TM 11 of *Ec*NhaA, although again, amino acid identity between the two proteins is low (16).

The structure of several TM fragments of *Sp*NHE1 has been deduced by NMR. We (56) recently demonstrated that there are many critical residues present within amino acids 360–378 and a similarity to TM 11 of *Ec*NhaA. Earlier (5), we also examined a putative TM segment of *Sp*NHE1 from amino acids 126 to 152. It also had similarity to TM 4 of NhaA and TM 4 of *h*NHE1 (see below).

Structural Basis of pH Modulation of *Sp*NHE1

There is substantial variation in pH profiles of plasma membrane Na^+/H^+ antiporters of different types. *Ec*NhaA primarily works at alkaline pH (>7.5) to extrude one Na^+ in exchange for two H^+. *Mj*NhaP1 and *h*NHE1 show a pH profile similar to each other and are more active at acidic intracellular pH. Their physiological functions are also similar, that is, to take H^+ out of the cell in exchange for Na^+ (51,57). *Pa*NhaP has an even more acidic active pH range (58). *Cryptococcus neoformans* Nha1 is responsible for survival in acidic environments and the protein is active at pHs as low as 4.5 (59) and *Sp*NHE1 is also active at more acidic extracellular pHs, with an optimum at approximately pH 4.5–5.0 (4).

The molecular mechanism of these different pH profiles is of great interest. Calinescu et al. (57) suggested that the differences might be due to the structural properties of the protein, possibly at the substrate binding site. *Ec*NhaA is of great interest since it increases its activity by three orders of magnitude between external pH of 6.5 and of 8.5 and has a known crystal structure. Many experiments have revealed putative parts of the mechanism by which pH modulates its activity. pH-induced changes in TM 1 and 9 were identified by trypsin digestion, antibody binding and cryoelectron microscopy (reviewed in ref. (60)). Computational analysis (61) suggested a continuum dielectric model for electrostatic interactions in *Ec*NhaA structure in its closed conformation. Results proposed a pH sensor at the cytoplasmic funnel of the protein, separated by 15 A from the binding site of the NhaA-fold (60). Four clusters of 18 titratable groups were proposed to be critical in this regard. Residues Glu78, Arg81, Glu-82, Glu252, His253, and His256 are one part of one cluster located in close proximity to one side of the cytoplasmic funnel entrance of the antiporter. They are thought to play a role as part of the pH sensor (61). Sensor residues were suggested to undergo protonation and deprotonation reactions with conformational changes in the protein (60). Glu78 was proposed as a trigger of pH-dependent structural changes. Earlier, it was also suggested that a pH change at the pH sensor results in alteration of the protonation state at the entrance of the cytoplasmic passage eliciting the conformational changes that are transmitted to activate NhaA (10).

Quite recently, another study presented an alternative mechanism of pH regulation of *Ec*NhaA and transport. They suggested that Glu78 does not have a pKa in the physiological range, but that three histidines might collectively respond to pH signals (62). In their competitive binding model, a sodium and two protons compete for binding to the active site. As pH is increased to the activation pH, the net charge of the pH sensor residues decreases to negative, attracting a sodium ion into the funnel. Simultaneously, Asp164 releases the first proton that induces opening of the cytoplasmic gate. This allows the entrance of water and a sodium ion. These are captured by Asp164, which is immediately below the cytoplasmic gate, and then shared with Asp163 and Thr132. Sodium binding to Asp163 disrupts a salt bridge with Lys300. This destabilizes its charged state and leads to release of the second proton. This proton release triggers a conformational change, possibly bending TM 5, which may precede a large conformational transition to the outward-facing state of NhaA (62).

REVISITING THE *Sp*NHE1 MODEL

We (36) recently predicted that plant *At*SOS1 contains 13 TM segments and not 12, similar to *Tth*NapA (11), *Mj*NhaP1 (32), and *Pa*NhaP. We used a similar protocol to examine the putative topology of *Sp*NHE1. An alignment of *Sp*NHE1 with *Ec*NhaA, *Pa*NhaP, and other Na^+/H^+ antiporters is shown in Supporting Information Fig. S1. *Sp*NHE1 shares its lowest sequence identity with *Ec*NhaA (18%) and highest sequence identity with *Pa*NhaP (21%). In sequence alignment, 13 TM segments of *Pa*NhaP show a reasonable alignment with the corresponding TM segments of *Sp*NHE1 and key residues important for transporter activity are aligned and described below. Based on the prediction and alignment, we generated a homology model (Fig. 1B) of *Sp*NHE1 with *Pa*NhaP structure in MODELLER (63). The homology model was further energy minimized and clashes removed using the CHIRON server (64).

Figures 1A and 1B show the predicted topology and 3D structure of *Sp*NHE1. The first two predicted TM segments are 13–29 (out to in, o->i) and 36–51 (i->o). There are three positively charged residues between them. The third TM segment contains a weakly hydrophobic stretch of amino acids with 69–83 (o->i). Others have also assigned this corresponding region as a TM segment in yeast NHEs (7,65). Residues 93–125 (i->o) span TM-4. The fifth TM helix (o->i) is equivalent to TM 4 of *Ec*NhaA and is a discontinuous helix (130–139, 146–153) with an intervening extended region. TM 6 (i->o), TM-7 (o->i), TM 8 (i->o), TM 9 (o->i) contain residues 163–192, 200–239, 245–263, 267–274, respectively. TM 10 (i->o) and TM 11 (o->i) contain the residues 295–312 and 325–349, respectively. TM 12 (359–385, i->o) has a second discontinuous helix, which corresponds to TM 11 of *Ec*NhaA and *h*NHE1. TM-13 (o->i) spans from 407–434 and thus the C-terminal resides inside the cell. There has been little direct study of the topology of *Sp*NHE1. However, one report (66), suggested Ala119 is accessible from the exterior of the cell, which agrees with this model. Figure 1B shows the predicted 3D structure of *Sp*NHE1. Critical motifs are highlighted and discussed below.

CRITICAL MOTIFS OF *Sp*NHE1

^{173}EXXXND^{178} Motif

The cation proton antiporter type 2 (CPA2) family of Na^+/H^+ antiporters carries out electrogenic exchange of cations. *Ec*NhaA contains a pair of Asp residues (DD motif, ^{163}DD^{164}, Supporting Information Fig. S1), that is, regarded as characteristic of the CPA2 family (57). This Asp pair is predicted to be involved in the transport of the two protons in exchange for one sodium ion (57) and mutation of these residues

demonstrates they are essential for transport (67). A corresponding DD is found in *Tth*NapA (^{156}DD^{157}).

Although *Sp*NHE1 contains a pair of Asp residues (^{266}DD^{267}), they do not align with the corresponding DD motifs of *Ec*NhaA and *Tth*NapA (Supporting Information Fig. S1). Rather, another motif "ND" of yeast plasma membrane antiporters (^{177}ND^{178} in *Sp*NHE1) occupies that place (Supporting Information Fig. S1). This ND motif may be characteristic of the CPA1 family of antiporters, which are responsible for electroneutral exchange of ions (57). The Na^+/H^+ antiporters *h*NHE1 (^{266}ND^{267}), *Pa*NhaP (^{158}ND^{159}), *Mj*NhaP1 (^{160}ND^{161}), and *At*SOS1 (^{200}ND^{201}) contain this motif. Mutation of Asp161 of *Mj*NhaP1 (68) and Asp267 of *h*NHE1 (19) compromises activity.

An analysis of the effects of mutation of acidic residues in this general region of *Sp*NHE1 was published earlier (69). Interestingly, Asp145, Asp266, Asp267, and Asp173 were critical for proper function. Surprisingly, mutation of Asp178 did not impair function. Glu173 is upstream of the ND motif (Supporting Information Fig. S1) and mutation to Gln generated an inactive protein. The *Sp*NHE1 model (Fig. 1B) suggests that Glu173 may be near Asp178, possibly compensating for its loss.

An equivalent of Glu173 of *Sp*NHE1 is found in *h*NHE1 (Glu262) (19), *Pa*NhaP (Glu154) (32), and *Mj*NhaP1 (Glu156) (13) (Supporting Information Fig. S1) but not in *Tth*NapA (11) and *Ec*NhaA (10). Therefore, we propose, that for plant, yeast, mammalian, and archaebacteria the "ND" motif can be extended to "EXXXND".

TDPV Sequence

Threonine residues appear to have an important role in activity of plasma membrane Na^+/H^+ antiporters and are part of a large important motif. In *Zr*Sod2–22p, Thr141 and Ser150 are important in substrate recognition and transport (70). A reciprocal substitution of these amino acids altered cation specificity. The Thr residue is quite conserved in yeast and other species and forms part of a TDPV sequence (Supporting Information Fig. S1). In *Sp*NHE1, (5) the equivalent Thr144 is also important in transport. Mutation to Ala, Asp, or Lys had marked effects on activity, while a mutant with a Ser had partial activity toward lithium. This suggests that the specific polarity of the Thr hydroxyl side chain might be an important factor at this position that influences cation specificity. The alteration in specificity induced by a change to Ser, might be because Ser imposes a slightly different bend in an α helix (71). A recent Thallium bound structure of *Pa*NhaP (PDB 4CZA) suggests that Thr at this position is involved in metal ion coordination via its backbone carbonyl group (12).

Other parts of the TDPV sequence, are also important in function of *Sp*NHE1 and other related proteins. The mutation D145N of *Sp*NHE1 was detrimental to activity (3). Prolines are critical in protein structure and tend to be helix breakers (72). The mutation P146A was disruptive to activity and disrupts *Sp*NHE1 targeting and folding (73). Mutation of Pro146 to other amino acids was not as disruptive, possibly because mutation to alanine was more disruptive of the protein structure. A Pro introduced into an alpha helix causes a kink and leaves two backbone carbonyls free (74). The Pro residues in TM helices are often associated with a Ser or Thr residue (S/TxP motif) which accommodates the structural needs of proteins (75). The Ser or Thr residues also induce helical distortions of functional significance (71). Together the combination functions as a mechanism for structural adaptation of membrane proteins (75). This sequence appears well conserved in the yeast antiporters and occurs in plant and *M. jannaschii* (Supporting Information Fig. S1).

In *Zr*Sod2–22, mutation of the conserved Pro145 to Ser or Thr allowed transport of K^+, which is not normally transported, demonstrating a change in substrate specificity (76). Other amino acid substitutions were inhibitory to activity. *h*NHE1 only partially aligns with the TDPV sequence with Val present at the Thr position (Supporting Information Fig. S1). Analysis of *h*NHE1 ^{238}DPV^{240} has shown that neither Asp238 nor Pro239 are critical to activity (77). It may be that another motif serves a similar function in *h*NHE1 and indeed Pro residues 167 and 168 of TM 4 of *h*NHE1 have been shown to be critical in activity of the protein (72).

Val147 is the last conserved residue of the yeast "TDPV" motif and its mutation to either Ala or Leu in *Sp*NHE1 is deleterious for activity (5). Sequence alignment shows that the yeast antiporter proteins contain either Val or Ile at this position (Supporting Information Fig. S1). This amino acid has not been extensively studied.

Putative NhaA-like Motif of *Sp*NHE1

As noted above, the prediction of the structure of *Sp*NHE1 resulted in a model where TM 5 and TM 12 were structurally similar to TM 4 and TM 11 of *Ec*NhaA. Additionally, amino acid alignment associated these same residues (Supporting Information Fig. S1). NMR analysis of a TM 5 synthetic peptide (amino acids 130–153) showed that it had helical regions for amino acids 128–143 and 147–154, separated by an unwound region (5). This is in agreement with the model. As noted earlier, the unwound region contains four conserved amino acids Thr144, Asp145, Pro146, and Val147 that yield defective proteins when mutated to alanine (3,5,73).

Predicted TM 12 (amino acids 359–385) aligned with TM 11 of *Ec*NhaA (Supporting Information Fig. S1), the other half of the NhaA fold. NMR analysis of a peptide of this region indicated amino acids 360–365 had a helical propensity followed by an extended region over amino acids 366–374, and another helical region over amino acids 376–386 (56). The extended region contained amino acids ^{366}GHFGPIGVC^{374}, whereas for *h*NHE1 TM 11 and for *Ec*NhaA TM 11, the discontinuous helix regions contain five (^{455}GGLRG^{459}) and three (^{336}GIG^{338}) amino acids, respectively (10,16). This roughly agrees with the model (Fig. 1). The sequence ^{336}GIG^{338} aligns with ^{369}GPI^{371} in yeast antiporters, (followed by Gly^{372}) in *Sp*NHE1 (Supporting Information Fig. S1). Pro370 may provide a functionally significant break in the helical structure, although interestingly, it is not essential—mutation of this amino acid to Ala did not eliminate

activity (56). Notably, when Ile371 is mutated to Ala, the protein has severely defective activity.

The C-terminal half of TM-12 contains multiple hydrophobic residues including Met378, Leu381, Leu384, and Leu386. Mutation of these amino acids to alanine yielded defects of varying degree in Li and Na transport. The only conserved positively charged residue in this region, K383, is also critical to activity (56). The model of *Sp*NHE1 suggests that these residues might be engaged in hydrophobic interaction with other TM segment 3 and 10. Such interactions may be critical for transport activity or structure of the protein.

CRITICAL RESIDUES

Positively Charged Residues in TM Segments

Yeast plasma membrane Na^+/H^+ antiporters contain positively charged amino acids within their TM domain. Three such conserved residues in *Sp*NHE1 are Arg77, Arg341, and Arg342. Arg77 is within TM 3 (Figs. 1 and 1S). TM 3 is unique in that it contains two conserved charged residues within the membrane, Glu74 and Arg77. The predicted structure of *Sp*NHE1 (Fig. 1B) suggests that these residues are located at the same side of the helix, away from the protein core. TM-3 may be at the dimer interface and Glu74 and Arg77 could be involved in dimer interaction. They are, however, only conserved across yeast species (Supporting Information Fig. S1) and the role of these residues is yet to be determined.

Arg341 and Arg342 of *Sp*NHE1 are located in putative TM 11 (Fig. 1). Multiple sequence alignment shows that Arg341 aligned with Lys300 of *Ec*NhaA and Arg425 of *h*NHE1 (Supporting Information Fig. S1). When mutated to alanine, Lys300 of *Ec*NhaA and Arg425 of *h*NHE1 compromised activity of the proteins (78,79). Lys300 of *Ec*NhaA may be involved in pH regulation of the protein (79). However, there is controversy in the role of Lys300 in *Ec*NhaA. One study, based on molecular modeling, suggested Lys300 is involved in transporting one of the two protons of electrogenic *Ec*NhaA. It was modeled to be in a salt bridge with Asp163 and to then rotate away leading to disruption of the bridge. Sodium binding to Asp163 was thought to release a proton from Lys300 (62). However, a recent study (80) mutated Lys300 of *Ec*NhaA to several amino acids and showed that the absence of a protonatable residue did not prevent electrogenic transport. In contrast, mutation of the equivalent residue in *Tth*NapA (Lys305) caused a nonelectrogenic transport (81).

In the case of *h*NHE1, the residue equivalent to Lys300 of *Ec*NhaA is Arg425. It has been shown to be important in *h*NHE1 activity (79). However, it is not known whether it forms a salt bridge with any upstream acidic amino acids as is postulated for *Ec*NhaA (62)

It is noteworthy that yeast and fungi plasma membrane Na^+/H^+ antiporters contain an arginine at this position forming a pair, Arg341-Arg342 for *Sp*NHE1 (Supporting Information Fig. S1). One of the two may function in the same role is as the corresponding Lys300 role of *Ec*NhaA, but the role of the second arginine is as yet unknown. TM Arg residues can also be attracted to phospholipid head groups, form a salt bridge, and can impose a tilt on TM helices (82), although it is not known whether this occurs in *Sp*NHE1.

Histidine Residues

Histidine residues have been shown to be important in the function of Na^+/H^+ antiporters such as *Ec*NhaA (83). *Sp*NHE1 contains eight histidine residues. Among the eight, only two histidines are conserved in yeast, His367 and His424 (Supporting Information Fig. S1), and only changes to His367 produced effects on function. His367 substitutions to either Arg or Ala produce an inactive protein (4,56). As noted above, NMR spectroscopy revealed that this TM segment contains a short helical region at its N-terminal followed by an extended region and then a helical region. His367 is located just at the N-terminal edge of the extended region (56). Mutation to Asp shifted the pH optimum to a more alkaline pH (4). This was similar to experiments with His225 of *Ec*NhaA (84). The H367R and H367A mutants were inactive. It is intriguing that in some fungal plasma membrane antiporters and in plant SOS1, the corresponding position is replaced by aromatic amino acids (Supporting Information Fig. S1). The histidine imidazole ring is aromatic; our recent data have shown that the aromatic residue Trp could replace His367 of *Sp*NHE1 H367W (56). The interaction between an aromatic side chain and a neighboring side chains could thus be an important factor in the activity of the protein.

pH Sensor

Details of the pH sensor of *Sp*NHE1 and most of the other transporters are not known. ^{266}DD^{267} of *Sp*NHE1 is located on the TM-8-TM-9 extracellular loop in our model (Fig. 1) which could be a pH-sensing motif along the translocation pathway. The position of the motif is only conserved in yeast pm-NHEs (Supporting Information Fig. S1). We have earlier shown that both the aspartates are essential for *Sp*NHE1 activity (4,69).

FUTURE DIRECTIONS

*Sp*NHE1 serves as a useful model for salt tolerance proteins. It has similarities to a number of other plasma membrane Na^+/H^+ antiporters and some differences. A number of critical motifs are maintained that are characteristic of this protein and related proteins and include a TDPV motif, EXXXND motif and an NhaA fold, consisting of two crossed helices, both with a helical interruption mid membrane. Future studies could involve cryoelectron microscopy of this, and other members of this family of proteins.

ACKNOWLEDGEMENTS

This work was supported by a Natural Sciences and Engineering Research Council of Canada (NSERC) grant (2014-06564; to L.F.).

REFERENCES

[1] Arino, J., Ramos, J., and Sychrova, H. (2010) Alkali metal cation transport and homeostasis in yeasts. Microbiol. Mol. Biol. Rev. 74, 95–120.

[2] Jia, Z.-P., McCullough, N., Martel, R., Hemmingsen, S., and Young, P. G. (1992) Gene amplification at a locus encoding a putative Na^+/H^+ antiporter confers sodium and lithium tolerance in fission yeast. EMBO J. 11, 1631–1640.

[3] Wiebe, C. A., Rieder, C., Young, P. G., Dibrov, P., and Fliegel, L. (2003) Functional analysis of amino acids of the Na^+/H^+ exchanger that are important for proton translocation. Mol. Cell Biochem. 254, 117–124.

[4] Dibrov, P., Young, P. G., and Fliegel, L. (1998) Functional analysis of amino acid residues essential for activity in the Na^+/H^+ exchanger of fission yeast. Biochemistry 36, 8282–8288.

[5] Ullah, A., Kemp, G., Lee, B., Alves, C., Young, H., et al. (2013) Structural and functional analysis of transmembrane segment IV of the salt tolerance protein Sod2. J. Biol. Chem. 288, 24609–24624.

[6] Prior, C., Potier, S., Souciet, J. L., and Sychrova, H. (1996) Characterization of the NHA1 gene encoding a Na^+/H^+-antiporter of the yeast *Saccharomyces cerevisiae*. FEBS Lett. 387, 89–93.

[7] Kinclova-Zimmermannova, O., Falson, P., Cmunt, D., and Sychrova, H. (2015) A hydrophobic filter confers the cation selectivity of *Zygosaccharomyces rouxii* plasma-membrane Na^+/H^+ antiporter. J. Mol. Biol. 427, 1681–1694.

[8] Watanabe, Y., Miwa, S., and Tamai, Y. (1995) Characterization of Na^+/H^+ - antiporter gene closely related to the salt-tolerance of yeast *Zygosacchromyces rouxii*. Yeast 11, 829–838.

[9] Pribylova, L., Papouskova, K., Zavrel, M., Souciet, J. L., and Sychrova, H. (2006) Exploration of yeast alkali metal cation/H^+ antiporters: sequence and structure comparison. Folia Microbiol. (Praha) 51, 413–424.

[10] Hunte, C., Screpanti, E., Venturi, M., Rimon, A., Padan, E., et al. (2005) Structure of a Na^+/H^+ antiporter and insights into mechanism of action and regulation by pH. Nature 435, 1197–1202.

[11] Lee, C., Kang, H. J., von Ballmoos, C., Newstead, S., Uzdavinys, P., et al. (2013) A two-domain elevator mechanism for sodium/proton antiport. Nature 501, 573–577.

[12] Paulino, C., and Kuhlbrandt, W. (2014) pH- and sodium-induced changes in a sodium/proton antiporter. Elife 3, e01412.

[13] Wohlert, D., Kuhlbrandt, W., and Yildiz, O. (2014) Structure and substrate ion binding in the sodium/proton antiporter PaNhaP. Elife 3, e03579.

[14] Alves, C., Lee, B. L., Sykes, B. D., and Fliegel, L. (2014) Structural and functional analysis of the transmembrane segment pair VI and VII of the NHE1 isoform of the Na^+/H^+ exchanger. Biochemistry 53, 3658–3670.

[15] Tzeng, J., Lee, B. L., Sykes, B. D., and Fliegel, L. (2010) Structural and functional analysis of transmembrane segment VI of the NHE1 isoform of the Na^+/H^+ exchanger. J. Biol. Chem. 285, 36656–36665.

[16] Lee, B. L., Li, X., Liu, Y., Sykes, B. D., and Fliegel, L. (2009) Structural and functional analysis of transmembrane XI of the NHE1 isoform of the Na^+/H^+ exchanger. J. Biol. Chem. 284, 11546–11556.

[17] Slepkov, E. R., Rainey, J. K., Li, X., Liu, Y., Cheng, F. J., et al. (2005) Structural and functional characterization of transmembrane segment IV of the NHE1 isoform of the Na^+/H^+ exchanger. J. Biol. Chem. 280, 17863–17872.

[18] Reddy, T., Ding, J., Li, X., Sykes, B. D., Rainey, J. K., et al. (2008) Structural and functional characterization of transmembrane segment IX of the NHE1 isoform of the Na^+/H^+ exchanger. J. Biol. Chem. 283, 22018–22030.

[19] Ding, J., Rainey, J. K., Xu, C., Sykes, B. D., and Fliegel, L. (2006) Structural and functional characterization of transmembrane segment VII of the Na^+/H^+ exchanger isoform 1. J. Biol. Chem. 281, 29817–29829.

[20] Wang, W., Vinocur, B., and Altman, A. (2003) Plant responses to drought, salinity and extreme temperatures: towards genetic engineering for stress tolerance. Planta 218, 1–14.

[21] Frommer, W. B., Ludewig, U., and Rentsch, D. (1999) Taking transgenic plants with a pinch of salt. Science 285, 1222–1223.

[22] Gao, X., Ren, Z., Zhao, Y., and Zhang, H. (2003) Overexpression of SOD2 increases salt tolerance of Arabidopsis. Plant Physiol. 133, 1873–1881.

[23] Brett, C. L., Donowitz, M., and Rao, R. (2005) Evolutionary origins of eukaryotic sodium/proton exchangers. Am. J. Physiol. Cell Physiol. 288, C223–C239.

[24] Kinclova, O., Potier, S., and Sychrova, H. (2002) Difference in substrate specificity divides the yeast alkali-metal-cation/H(+) antiporters into two subfamilies. Microbiology 148, 1225–1232.

[25] Kojima, A., Toshima, J. Y., Kanno, C., Kawata, C., and Toshima, J. (2012) Localization and functional requirement of yeast Na^+/H^+ exchanger, Nhx1p, in the endocytic and protein recycling pathway. Biochim. Biophys. Acta 1823, 534–543.

[26] Brett, C. L., Tukaye, D. N., Mukherjee, S., and Rao, R. (2005) The yeast endosomal Na^+K^+/H^+ exchanger Nhx1 regulates cellular pH to control vesicle trafficking. Mol. Biol. Cell 16, 1396–1405.

[27] Zhu, J., Ying, S. H., and Feng, M. G. (2016) The Na^+/H^+ antiporter Nhx1 controls vacuolar fusion indispensible for life cycles in vitro and in vivo in a fungal insect pathogen. Environ. Microbiol. 18, 3884–3895.

[28] Wells, K. M., and Rao, R. (2001) The yeast Na^+/H^+ exchanger Nhx1 is an N-linked glycoprotein. Topological implications. J. Biol. Chem. 276, 3401–3407.

[29] Kinclova, O., Potier, S., and Sychrova, H. (2001) The *Zygosaccharomyces rouxii* strain CBS732 contains only one copy of the HOG1 and the SOD2 genes. J. Biotechnol. 88, 151–158.

[30] Papouskova, K., and Sychrova, H. (2007) *Schizosaccharomyces pombe* possesses two plasma membrane alkali metal cation/H antiporters differing in their substrate specificity. FEMS Yeast Res. 7, 188–195.

[31] Padan, E. (2014) Functional and structural dynamics of NhaA, a prototype for Na(+) and H(+) antiporters, which are responsible for Na(+) and H(+) homeostasis in cells. Biochim. Biophys. Acta 1837, 1047–1062.

[32] Goswami, P., Paulino, C., Hizlan, D., Vonck, J., Yildiz, O., et al. (2011) Structure of the archaeal Na^+/H^+ antiporter NhaP1 and functional role of transmembrane helix 1. EMBO J. 30, 439–449.

[33] Wakabayashi, S., Pang, T., Su, X., and Shigekawa, M. (2000) A novel topology model of the human Na^+/H^+ exchanger isoform 1. J. Biol. Chem. 275, 7942–7949.

[34] Landau, M., Herz, K., Padan, E., and Ben-Tal, N. (2007) Model structure of the Na^+/H^+ exchanger 1 (NHE1): functional and clinical implications. J. Biol. Chem. 282, 37854–37863.

[35] Liu, Y., Basu, A., Li, X., and Fliegel, L. (2015) Topological analysis of the Na/H exchanger. Biochim. Biophys. Acta 1848, 2385–2393.

[36] Ullah, A., Dutta, D., and Fliegel, L. (2016) Expression and characterization of the SOS1 Arabidopsis salt tolerance protein. Mol. Cell Biochem. 415, 133–143.

[37] Hendus-Altenburger, R., Kragelund, B. B., and Pedersen, S. F. (2014) Structural dynamics and regulation of the mammalian SLC9A family of Na(+)/H(+) exchangers. Curr. Top. Membr. 73, 69–148.

[38] Padan, E., Danieli, T., Keren, Y., Alkoby, D., Masrati, G., et al. (2015) NhaA antiporter functions using 10 helices, and an additional 2 contribute to assembly/stability. Proc. Natl. Acad. Sci. USA 112, E5575–E5582. PMC][10.1073/pnas.1510964112] [26417087]

[39] Rimon, A., Tzubery, T., and Padan, E. (2007) Monomers of the NhaA Na^+/H^+ antiporter of *Escherichia coli* are fully functional yet dimers are beneficial under extreme stress conditions at alkaline pH in the presence of Na^+ or Li^+. J. Biol. Chem. 282, 26810–26821.

[40] Fafournoux, P., Noel, J., and Pouysségur, J. (1994) Evidence that Na^+/H^+ exchanger isoforms NHE1 and NHE3 exist as stable dimers in membranes with a high degree of specificity for homodimers. J. Biol. Chem. 269, 2589–2596.

[41] Moncoq, K., Kemp, G., Li, X., Fliegel, L., and Young, H. S. (2008) Dimeric structure of human Na^+/H^+ exchanger isoform 1 overproduced in *Saccharomyces cerevisiae*. J. Biol. Chem. 283, 4145–4154.

[42] Nunez-Ramirez, R., Sanchez-Barrena, M. J., Villalta, I., Vega, J. F., Pardo, J. M., et al. (2012) Structural insights on the plant salt-overly-sensitive 1 (SOS1) Na(+)/H(+) antiporter. J. Mol. Biol. 424, 283–294.

[43] Chen, H., and Fliegel, L. (2008) Expression, purification, and reconstitution of the Na(+)/H (+) exchanger sod2 in *Saccharomyces cerevisiae*. Mol. Cell Biochem. 319, 79–90.

[44] Kinclova, O., Ramos, J., Potier, S., and Sychrova, H. (2001) Functional study of the *Saccharomyces cerevisiae* Nha1p C-terminus. Mol. Microbiol. 40, 656–668.

[45] Kamauchi, S., Mitsui, K., Ujike, S., Haga, M., Nakamura, N., et al. (2002) Structurally and functionally conserved domains in the diverse hydrophilic

carboxy-terminal halves of various yeast and fungal na/h antiporters (nha1p). J. Biochem. (Tokyo) 131, 821–831.
[46] Mitsui, K., Kamauchi, S., Nakamura, N., Inoue, H., and Kanazawa, H. (2004) A conserved domain in the tail region of the *Saccharomyces cerevisiae* Na^+/H^+ antiporter (Nha1p) plays important roles in localization and salinity-resistant cell-growth. J. Biochem. 135, 139–148.
[47] Proft, M., and Struhl, K. (2004) MAP kinase-mediated stress relief that precedes and regulates the timing of transcriptional induction. Cell 118, 351–361.
[48] Zahradka, J., van Heusden, G. P., and Sychrova, H. (2012) Yeast 14-3-3 proteins participate in the regulation of cell cation homeostasis via interaction with Nha1 alkali-metal-cation/proton antiporter. Biochim. Biophys. Acta 1820, 849–858.
[49] Mitsui, K., Ochi, F., Nakamura, N., Doi, Y., Inoue, H., et al. (2004) A novel membrane protein capable of binding the Na^+/H^+ antiporter (Nha1p) enhances the salinity-resistant cell growth of *Saccharomyces cerevisiae*. J. Biol. Chem. 279, 12438–12447.
[50] Quintero, F. J., Martinez-Atienza, J., Villalta, I., Jiang, X., Kim, W. Y., et al. (2011) Activation of the plasma membrane Na/H antiporter Salt-Overly-Sensitive 1 (SOS1) by phosphorylation of an auto-inhibitory C-terminal domain. Proc. Natl. Acad. Sci. USA 108, 2611–2616.
[51] Odunewu-Aderibigbe, A., and Fliegel, L. (2014) The Na(+)/H(+) exchanger and pH regulation in the heart. IUBMB Life 66, 679–685.
[52] Hendus-Altenburger, R., Lambrughi, M., Terkelsen, T., Pedersen, S. F., Papaleo, E., et al. (2017) A phosphorylation-motif for tuneable helix stabilisation in intrinsically disordered proteins - Lessons from the sodium proton exchanger 1 (NHE1). Cell Signal 37, 40–51.
[53] Wiebe, C. A., Dibattista, E. R., and Fliegel, L. (2001) Functional role of polar amino acid residues in Na^+/H^+ exchangers. Biochem. J. 357, 1–10.
[54] Rimon, A., Kozachkov-Magrisso, L., and Padan, E. (2012) The unwound portion dividing helix IV of NhaA undergoes a conformational change at physiological pH and lines the cation passage. Biochemistry 51, 9560–9569.
[55] Lee, B. L., Sykes, B. D., and Fliegel, L. (2013) Structural and functional insights into the cardiac Na(+)/H(+) exchanger. J. Mol. Cell Cardiol. 61, 60–67.
[56] Dutta, D., Shin, K., Rainey, J. K., and Fliegel, L. (2017) Transmembrane segment XI of the Na^+/H^+ antiporter of *S. pombe* is a critical part of the ion translocation pore. Sci. Rep. 7, 12793.
[57] Calinescu, O., Paulino, C., Kuhlbrandt, W., and Fendler, K. (2014) Keeping it simple, transport mechanism and pH regulation in Na^+/H^+ exchangers. J. Biol. Chem. 289, 13168–13176.
[58] Calinescu, O., Linder, M., Wohlert, D., Yildiz, O., Kuhlbrandt, W., et al. (2016) Electrogenic Cation Binding in the Electroneutral Na^+/H^+ Antiporter of Pyrococcus abyssi. J. Biol. Chem. 291, 26786–26793.
[59] Jung, K. W., Strain, A. K., Nielsen, K., Jung, K. H., and Bahn, Y. S. (2012) Two cation transporters Ena1 and Nha1 cooperatively modulate ion homeostasis, antifungal drug resistance, and virulence of Cryptococcus neoformans via the HOG pathway. Fungal Genet. Biol. 49, 332–345.
[60] Krulwich, T. A., Sachs, G., and Padan, E. (2011) Molecular aspects of bacterial pH sensing and homeostasis. Nat. Rev. Microbiol. 9, 330–343.
[61] Olkhova, E., Hunte, C., Screpanti, E., Padan, E., and Michel, H. (2006) Multiconformation continuum electrostatics analysis of the NhaA Na^+/H^+ antiporter of *Escherichia coli* with functional implications. Proc. Natl. Acad. Sci. USA 103, 2629–2634.
[62] Huang, Y., Chen, W., Dotson, D. L., Beckstein, O., and Shen, J. (2016) Mechanism of pH-dependent activation of the sodium-proton antiporter NhaA. Nat. Commun. 7, 12940.
[63] Sali, A., and Blundell, T. L. (1993) Comparative protein modelling by satisfaction of spatial restraints. J. Mol. Biol. 234, 779–815.
[64] Ramachandran, S., Kota, P., Ding, F., and Dokholyan, N. V. (2011) Automated minimization of steric clashes in protein structures. Proteins 79, 261–270.
[65] Sato, Y., and Sakaguchi, M. (2005) Topogenic properties of transmembrane segments of *Arabidopsis thaliana* NHX1 reveal a common topology model of the Na^+/H^+ exchanger family. J. Biochem. (Tokyo) 138, 425–431.
[66] Ullah, A., El-Magd, R. A., and Fliegel, L. (2014) Functional role and analysis of cysteine residues of the salt tolerance protein Sod2. Mol. Cell Biochem. 386, 85–98.
[67] Padan, E., Kozachkov, L., Herz, K., and Rimon, A. (2009) NhaA crystal structure: functional-structural insights. J. Expl. Biol. 212, 1593–1603.
[68] Hellmer, J., Teubner, A., and Zeilinger, C. (2003) Conserved arginine and aspartate residues are critical for function of MjNhaP1, a Na^+/H^+ antiporter of M. jannaschii. FEBS Lett. 542, 32–36.
[69] Fliegel, L. (2005) Identification of conserved polar residues important for salt tolerance by the Na^+/H^+ exchanger of *Schizosaccharomyces pombe*. Mol. Cell Biochem. 268, 83–92.
[70] Kinclova-Zimmermannova, O., Zavrel, M., and Sychrova, H. (2006) Importance of the seryl and threonyl residues of the fifth transmembrane domain to the substrate specificity of yeast plasma membrane Na^+/H^+ antiporters. Mol. Membr. Biol. 23, 349–361.
[71] Ballesteros, J. A., Deupi, X., Olivella, M., Haaksma, E. E., and Pardo, L. (2000) Serine and threonine residues bend alpha-helices in the chi(1) = g(-) conformation. Biophys. J. 79, 2754–2760.
[72] Slepkov, E. R., Chow, S., Lemieux, M. J., and Fliegel, L. (2004) Proline residues in transmembrane segment IV are critical for activity, expression and targeting of the Na^+/H^+ exchanger isoform 1. Biochem. J. 379, 31–38.
[73] Ndayizeye, M., Touret, N., and Fliegel, L. (2009) Proline 146 is critical to the structure, function and targeting of sod2, the Na^+/H^+ exchanger of *Schizosaccharomyces pombe*. Biochim. Biophys. Acta 1788, 983–992.
[74] Sansom, M. S. (1992) Proline residues in transmembrane helices of channel and transport proteins: a molecular modelling study. Protein Eng. 5, 53–60.
[75] Deupi, X., Olivella, M., Govaerts, C., Ballesteros, J. A., Campillo, M., and Pardo, L. (2004) Ser and Thr residues modulate the conformation of prokinked transmembrane alpha-helices. Biophys. J. 86, 105–115.
[76] Kinclova-Zimmermannova, O., Zavrel, M., and Sychrova, H. (2005) Identification of conserved prolyl residue important for transport activity and the substrate specificity range of yeast plasma membrane Na^+/H^+ antiporters. J. Biol. Chem. 280, 30638–30647.
[77] Murtazina, R., Booth, B. J., Bullis, B. L., Singh, D. N., and Fliegel, L. (2001) Functional analysis of polar amino-acid residues in membrane associated regions of the NHE1 isoform of the mammalian Na^+/H^+ exchanger. Eur. J. Biochem. 268, 4674–4685.
[78] Maes, M., Rimon, A., Kozachkov-Magrisso, L., Friedler, A., and Padan, E. (2012) Revealing the ligand binding site of NhaA Na^+/H^+ antiporter and its pH dependence. J. Biol. Chem. 287, 38150–38157.
[79] Li, X., Ma, Y., and Fliegel, L. (2014) Functional role of arginine 425 in the mammalian Na(+)/H(+) exchanger. Biochem. Cell Biol. 92, 541–546.
[80] Calinescu, O., Dwivedi, M., Patino-Ruiz, M., Padan, E., and Fendler, K. (2017) Lysine300 is essential for stability but not for electrogenic transport of the *E. coli* NhaA Na^+/H^+ antiporter. J. Biol. Chem. 292, 7932–7941.
[81] Uzdavinys, P., Coincon, M., Nji, E., Ndi, M., Winkelmann, I., et al. (2017) Dissecting the proton transport pathway in electrogenic Na^+/H^+ antiporters. Proc. Natl. Acad. Sci. USA 114, E1101–E1110.
[82] Norimatsu, Y., Hasegawa, K., Shimizu, N., and Toyoshima, C. (2017) Protein-phospholipid interplay revealed with crystals of a calcium pump. Nature 545, 193–198.
[83] Gerchman, Y., Olami, Y., Rimon, A., Taglicht, D., Schuldiner, S., et al. (1993) Histidine-226 is part of the pH sensor of NhaA, a Na^+/H^+ antiporter in *Escherichia coli*. Proc. Natl. Acad. Sci. USA 90, 1212–1216.
[84] Rimon, A., Gershman, Y., Olami, Y., Schuldiner, S., and Padan, E. (1995) Replacements of histidine 226 of NhaA-Na^+/H^+ antiporter of *Escherichia coli*. Cysteine (H226C) or serine (H226S) retain both normal activity and pH sensitivity, aspartate (H226D) shifts the pH profile toward basic pH, and alanine (H226A) inactivates the carrier at all pH values. J. Biol. Chem. 270, 26813–26817.